PHYSICAL REVIEW D **92,** 114027 (2015)

Entanglement interaction and the phase diagram of strongly interacting matter

G. Y. Shao,[1] Z. D. Tang,[1] M. Di Toro,[2,3] M. Colonna,[2] X. Y. Gao,[1] N. Gao,[1] and Y. L. Zhao[4]

[1]*Department of Applied Physics, Xi'an Jiaotong University, Xi'an 710049, China*
[2]*INFN-Laboratori Nazionali del Sud, Via S. Sofia 62, Catania I-95123, Italy*
[3]*Physics and Astronomy Dept., University of Catania, Via S. Sofia 64, Catania I-95123, Italy*
[4]*School of Energy and Power Engineering, Xi'an Jiaotong University, Xi'an 710049, China*

(Received 15 October 2015; published 23 December 2015)

The entanglement interactions between the Polyakov loop and chiral condensate have been recently studied in the entangled Polyakov-loop Nambu–Jona-Lasinio model (EPNJL). The calculation shows that such an interaction plays an important role in the pseudocritical temperatures of deconfinement and chiral symmetry restoration. As a further study, here we construct a hadron-quark two-equation-of-state (two-EoS) model, based on the Walecka-quantum hadrodynamics and the EPNJL pictures, in order to study the equilibrium transition between hadronic and quark matter in heavy-ion collisions at finite densities and temperatures. We can explore the phase diagram of strongly interacting matter and the transition boundaries from nuclear to quark matter. We discuss the influence of the entanglement interaction on the critical point of the expected first-order phase transition in the two-EoS model. In particular, for charge asymmetric matter, we analyze the local asymmetry of the u, d quarks as a function of quark concentration in the hadron-quark mixed phase during the phase transition. We finally propose some related observables that are possibly measurable in heavy-ion collision experiments.

DOI: 10.1103/PhysRevD.92.114027 PACS numbers: 12.38.Mh, 25.75.Nq

I. INTRODUCTION

The exploration of the QCD phase diagram of strongly interacting matter and the phase transition signatures from nuclear to quark-gluon matter are subjects of great interest in recent decades. The investigation involves ultrarelativistic heavy-ion collisions (HICs), nuclear astrophysics, and the evolution of the early Universe. Intensive searches with high-energy HICs have been performed at laboratories, such as the Relativistic Heavy Ion Collider (RHIC) and the Large Hadron Collider (LHC), and a promising observation of the signatures of the phase transformation is eagerly anticipated [1]. On the other hand, observations from compact stars [2–4] gradually provide us more and more important data in exploring the properties of strongly interacting matter.

However, in spite of tremendous theoretical and experimental efforts, the QCD phase diagram has not been unveiled yet [5,6]. As a fundamental tool, lattice QCD (l-QCD) simulation provides us a good framework to investigate the thermodynamics of strongly interacting matter at small chemical potential [7–12], but it suffers the well-known sign problem of the fermion determinant with three colors at finite baryon chemical potential. Though some approximation methods have been proposed to try to evade the problem, the region of large densities and low temperatures essentially remains inaccessible [13–16].

To give a complete description of the QCD phase diagram, different types of quantum field theory approaches and phenomenological models, such as the Dyson-Schwinger equation approach [17–24], the Nambu–Jona-Lasinio (NJL) model [25–36], the Polyakov-loop improved NJL (PNJL) model [37–46], and the Polyakov-loop extended quark meson (PQM) model [47–49], have been developed to disclose the essence of strong interaction. Among these models, the PNJL model, which takes into account both the chiral symmetry and (de)confinement effect, gives a good presentation of lattice data at high temperatures. At the same time, it has the ability to make predictions at high baryon density that cannot be reached presently in l-QCD simulations.

As a further improvement, the PNJL model has been generalized recently to include an effective four-quark vertex interaction coupled with a Poyakov loop, the entanglement interaction. The extension of the PNJL model with the entanglement interaction between the chiral condensate and Polyakov loop is named the EPNJL model [50–52]. In the EPNJL model, the entanglement correlates the quark chiral symmetry and color confinement, which plays an important role in the properties of quark-gluon matter at high temperature and low chemical potentials. With such an entanglement interaction, the coincidence of chiral symmetry restoration and quark deconfinement can be easily obtained with adapted parameters. Recently, the theta-vacuum effects on the QCD phase diagram were also studied using the SU(3) EPNJL model in [53]. In addition, it was taken to explore the phase diagram for zero and imaginary quark-number chemical potential in [54] to reproduce qualitatively the lattice QCD results. In Refs. [55,56], the effect of external magnetic field on the deconfinement and chiral pseudocritical temperatures was also investigated in the EPNJL model.

Most effective models, including the (E)PNJL model, describe strongly interacting matter based on quark degrees of freedom. Baryons are not treated in these models. However, as far as we know, the QCD dynamics is governed by hadrons at low temperatures and relatively small baryon chemical potentials. When one investigates the phase transformation from nuclear to quark matter, it is practical and plausible to describe nuclear matter based on the hadronic degrees of freedom at low T and small μ_B, but quark matter with quark degrees of freedom at high T and large μ_B. This picture can be realized in an equilibrium phase transition between the hadronic and quark phases, possibly reached in the interior of compact stars and in HIC experiments at intermediate energies.

In the equilibrium transition from hadronic to quark matter, the two phases are connected through the Gibbs conditions. This approach is widely used in the description of the phase transition in a neutron star with a quark core or kaon condensate [57–66]. Recently, this method has been generalized to explore the phase diagram of the hadron-quark phase transition in HICs [67–76]. In particular, attention was focused on the isospin asymmetric matter, and some observable isospin effects on charged meson yield ratios were proposed in our previous investigations [74–76].

As a further study along this line, we construct a new two-EoS model based on the recently developed EPNJL model and explore the phase diagram of strongly interacting matter with an equilibrium phase transition. We investigate the influence of the entanglement interaction on the location of the critical point of the first-order phase transition and propose some observables relevant in the transformation from asymmetric nuclear matter to quark matter. This study can be significant for the planned subjects at the new facilities of NICA (JINR-Dubna) and FAIR (GSI-Darmstadt) as well as for the beam energy scan (BES) program at RHIC, with realistic asymmetries for stable and unstable nuclei.

The paper is organized as follows. In Sec. II, we describe briefly the two-EoS approach and give the relevant formulas of the hadron-EPNJL model. In Sec. III, we present the numerical results about the phase diagram of the equilibrated phase transition and propose some possible observables to explore the transition boundaries from asymmetric nuclear matter to quark matter in HICs. Finally, a summary and some suggestions for further study are given in Sec. IV.

II. THE MODELS

In the two-EoS model, the pure hadronic phase at low T and small μ_B is described by the nonlinear Walecka-type model. The pure quark phase at high T and large μ_B is described with the EPNJL model with the entanglement interaction between the chiral condensate and Poyakov loop. For the phase transition from nuclear matter to quark matter, the phases are connected through the Gibbs conditions with thermal, chemical, and mechanical equilibrium. In addition, the asymmetry parameters in the hadron-quark mixed phase are required to fulfill the isospin charge conservation in strong interaction.

A. The pure hadronic matter

To describe nuclear matter, we take the Lagrangian,

$$\begin{aligned}\mathcal{L}^H = &\sum_N \bar{\psi}_N[i\gamma_\mu\partial^\mu - M + g_\sigma\sigma - g_\omega\gamma_\mu\omega^\mu - g_\rho\gamma_\mu\boldsymbol{\tau}\cdot\boldsymbol{\rho}^\mu]\psi_N \\ &+\frac{1}{2}(\partial_\mu\sigma\partial^\mu\sigma - m_\sigma^2\sigma^2) - V(\sigma) + \frac{1}{2}m_\omega^2\omega_\mu\omega^\mu \\ &-\frac{1}{4}\omega_{\mu\nu}\omega^{\mu\nu} + \frac{1}{2}m_\rho^2\boldsymbol{\rho}_\mu\cdot\boldsymbol{\rho}^\mu - \frac{1}{4}\boldsymbol{\rho}_{\mu\nu}\cdot\boldsymbol{\rho}^{\mu\nu}, \end{aligned} \tag{1}$$

where $\omega_{\mu\nu} = \partial_\mu\omega_\nu - \partial_\nu\omega_\mu$, $\rho_{\mu\nu} \equiv \partial_\mu\boldsymbol{\rho}_\nu - \partial_\nu\boldsymbol{\rho}_\mu$. In this model, the interactions between nucleons are mediated by σ, ω, ρ mesons. The self-interactions of the σ meson, $V(\sigma) = \frac{1}{3}b(g_\sigma\sigma)^3 + \frac{1}{4}c(g_\sigma\sigma)^4$, are included to give the correct compression modulus, the effective nucleon mass at saturation density. The parameter set NL3 is used in the calculation, which gives a well description of the properties of nuclear matter. (The details can be found in Refs. [57,63]).

To describe asymmetric nuclear matter, we define the baryon and isospin chemical potential as $\mu_B^H = (\mu_p + \mu_n)/2$, $\mu_3^H = (\mu_p - \mu_n)$, The asymmetry parameter is defined as

$$\alpha^H = (\rho_n - \rho_p)/(\rho_p + \rho_n), \tag{2}$$

which is determined by the heavy ions taken in experiments. The values of α^H are compiled for some heavy-ion sources in [72], and the largest one is $\alpha^H = 0.227$ in $^{238}\mathrm{U} + ^{238}\mathrm{U}$ collision for stable nuclei. For unstable nuclei, α^H can take a larger value.

B. The pure quark matter

We describe pure quark matter using the recently developed EPNJL model [50,51]. Firstly, we introduce the PNJL model, and then consider the entanglement interaction between chiral condensate and Poyakov loop. The Lagrangian of the standard two-flavor PNJL model is

$$\begin{aligned}\mathcal{L}^Q = &\bar{q}(i\gamma^\mu D_\mu - \hat{m}_0)q + G(\Phi)[(\bar{q}q)^2 + (\bar{q}i\gamma_5\vec{\tau}q)^2] \\ &-\mathcal{U}(\Phi[A], \bar{\Phi}[A], T), \end{aligned} \tag{3}$$

where q denotes the quark fields with two flavors, u and d, and three colors; $\hat{m}_0 = \mathrm{diag}(m_u, m_d)$ in flavor space. The covariant derivative in the Lagrangian is defined as $D_\mu = \partial_\mu - iA_\mu - i\mu_q\delta_\mu^0$. The gluon background field $A_\mu = \delta_\mu^0 A_0$ is supposed to be homogeneous and static, with $A_0 = g\mathcal{A}_0^\alpha\frac{\lambda^\alpha}{2}$, where $\frac{\lambda^\alpha}{2}$ is the $SU(3)$ color generators.

The effective potential $\mathcal{U}(\Phi[A],\bar{\Phi}[A],T)$ is expressed in terms of the traced Polyakov loop $\Phi=(\mathrm{Tr}_c L)/N_C$ and its conjugate $\bar{\Phi}=(\mathrm{Tr}_c L^\dagger)/N_C$. The Polyakov loop L is a matrix in color space,

$$L(\vec{x})=\mathcal{P}\exp\left[i\int_0^\beta d\tau A_4(\vec{x},\tau)\right], \tag{4}$$

where $\beta=1/T$ is the inverse of temperature and $A_4=iA_0$. The temperature-dependent effective potential $\mathcal{U}(\Phi,\bar{\Phi},T)$ proposed in [77] to mimic Lattice QCD data is taken in this study, with the form

$$\frac{\mathcal{U}(\Phi,\bar{\Phi},T)}{T^4}=-\frac{a(T)}{2}\bar{\Phi}\Phi+b(T)\ln[1-6\bar{\Phi}\Phi+4(\bar{\Phi}^3+\Phi^3)-3(\bar{\Phi}\Phi)^2], \tag{5}$$

where

$$a(T)=a_0+a_1\left(\frac{T_0}{T}\right)+a_2\left(\frac{T_0}{T}\right)^2,\qquad b(T)=b_3\left(\frac{T_0}{T}\right)^3. \tag{6}$$

The parameters a_i, b_i summarized in Table I are precisely fitted according to the result of l-QCD thermodynamics in the pure gauge sector. And T_0 is found to be 270 MeV as the critical temperature for the deconfinement phase transition at zero baryon chemical potential [78]. When fermion fields are included, a rescaling of T_0 is usually implemented to obtain a consistent result between the model calculation and full lattice simulation which gives the critical temperatures of deconfinement $T_\Phi=173\pm 8$ MeV [7–9] at zero chemical potential.

In the PNJL model, $T_0=210$ MeV is usually taken in the literature, which produces the pseudocritical temperature of chiral symmetry restoration $T_\sigma=205.1$ and $T_\Phi=172.7$ MeV. The difference $\Delta=|T_\sigma-T_\Phi|/T_\sigma$ is about 15%. However, according to the Coleman-Witten conjecture, it has long been believed that chiral symmetry restoration and color deconfinement have a common origin, and the associated phase transitions coincide. The coincidence has been reproduced in some practical calculation of l-QCD at imaginary chemical potential and at real and imaginary isospin chemical potential where the sign problem does not appear. The coincidence cannot be reproduced in the original PNJL model. This shortcoming of the PNJL model comes from the weak correlation between the chiral condensate and the quark Poyakov loop. To evade this problem, an effective four-quark vertex $G(\Phi)$ depending on Φ is introduced in [50,51]

$$G(\Phi)=G[1-\alpha_1\Phi\bar{\Phi}-\alpha_2(\Phi^3+\bar{\Phi}^3)], \tag{7}$$

which preserves the chiral symmetry, the C symmetry, and the extended $\mathbb{Z}_3$ symmetry.

With the consideration of such an entanglement interaction between the chiral condensate and Poyakov loop, this model is named the EPNJL model. We then replace the four quark vertex, G, in the Largrangian given in Eq. (3) with the new vertex $G(\Phi)$.

The thermodynamical potential of quark matter in the EPNJL model within the mean field approximation can be derived then as

$$\begin{aligned}\Omega=&\,\mathcal{U}(\bar{\Phi},\Phi,T)+G(\Phi)(\phi_u+\phi_d)^2\\&-2\int_\Lambda\frac{\mathrm{d}^3\boldsymbol{k}}{(2\pi)^3}3(E_u+E_d)\\&-2T\sum_{u,d}\int\frac{\mathrm{d}^3\boldsymbol{k}}{(2\pi)^3}[\ln(1+3\Phi e^{-(E_i-\mu_i)/T}\\&+3\bar{\Phi}e^{-2(E_i-\mu_i)/T}+e^{-3(E_i-\mu_i)/T})]\\&-2T\sum_{u,d}\int\frac{\mathrm{d}^3\boldsymbol{k}}{(2\pi)^3}[\ln(1+3\bar{\Phi}e^{-(E_i+\mu_i)/T}\\&+3\Phi e^{-2(E_i+\mu_i)/T}+e^{-3(E_i+\mu_i)/T})],\end{aligned} \tag{8}$$

where $E_i=\sqrt{\boldsymbol{k}^2+M_i^2}$ is the energy-momentum dispersion relation of the quark flavor i, and μ_i is the corresponding quark chemical potential.

The dynamical quark masses and quark condensates are coupled with the following equations,

$$M_i=m_0-2G(\Phi)(\phi_u+\phi_d), \tag{9}$$

$$\phi_i=-2N_c\int\frac{d^3\boldsymbol{k}}{(2\pi)^3}\frac{M_i}{E_i}(1-n_i(k)-\bar{n}_i(k)), \tag{10}$$

where $n_i(k)$ and $\bar{n}_i(k)$

$$n_i(k)=\frac{\Phi e^{-(E_i-\mu_i)/T}+2\bar{\Phi}e^{-2(E_i-\mu_i)/T}+e^{-3(E_i-\mu_i)/T}}{1+3\Phi e^{-(E_i-\mu_i)/T}+3\bar{\Phi}e^{-2(E_i-\mu_i)/T}+e^{-3(E_i-\mu_i)/T}}, \tag{11}$$

$$\bar{n}_i(k)=\frac{\bar{\Phi}e^{-(E_i+\mu_i)/T}+2\Phi e^{-2(E_i+\mu_i)/T}+e^{-3(E_i+\mu_i)/T}}{1+3\bar{\Phi}e^{-(E_i+\mu_i)/T}+3\Phi e^{-2(E_i+\mu_i)/T}+e^{-3(E_i+\mu_i)/T}}. \tag{12}$$

are modified Fermion distribution functions of quark and antiquark. The values of ϕ_u, ϕ_d, Φ, and $\bar{\Phi}$ can be determined by minimizing the thermodynamical potential,

TABLE I. Parameters in Polyakov effective potential given in [77].

a_0	a_1	a_2	b_3
3.51	−2.47	15.2	−1.75

$$\frac{\partial\Omega}{\partial\phi_u}=\frac{\partial\Omega}{\partial\phi_d}=\frac{\partial\Omega}{\partial\Phi}=\frac{\partial\Omega}{\partial\bar{\Phi}}=0. \tag{13}$$

All the thermodynamic quantities relevant to the bulk properties of quark matter can be obtained from Ω. In particular, we note that the pressure and energy density should be zero in the vacuum.

Like the NJL model, the EPNJL model is not renormalizeable, so a cutoff Λ is implemented in 3-momentum space for divergent integrations. Here $\Lambda = 651$ MeV, $G = 5.04$ GeV^{-2}, $m_{u,d} = 5.5$ MeV will be taken by fitting the experimental values of the pion decay constant $f_\pi = 92.3$ MeV and pion mass $m_\pi = 139.3$ MeV.

For asymmetric quark matter, the baryon and isospin chemical potential are defined as $\mu_B^Q = \frac{3}{2}(\mu_u + \mu_d)$, $\mu_3^Q = (\mu_u - \mu_d)$, respectively. The asymmetry parameter of pure quark matter is

$$\alpha^Q = -\frac{\rho_3^Q}{\rho_B^Q} = -\frac{(\rho_u - \rho_d)}{(\rho_u + \rho_d)/3}, \tag{14}$$

where $\rho_3^Q = (\rho_u - \rho_d)$, and $\rho_B^Q = (\rho_u + \rho_d)/3$.

C. The hadron-quark mixed phase

The above introduction is a separate description of the pure hadronic and quark phase. When the equilibrated phase transformation between the hadronic and quark matter forms, the Gibbs conditions (thermal, chemical, and mechanical equilibrium) need to be fulfilled (general discussion of phase transitions in multicomponent systems can be found in Ref. [58]),

$$\mu_B^H = \mu_B^Q, \qquad \mu_3^H = \mu_3^Q, \qquad T^H = T^Q, \qquad P^H = P^Q, \tag{15}$$

where μ_3^H and μ_3^Q are the isospin chemical potential of the two phases. For the coexisting phase, the total baryon density consists of two parts, $\rho_B = (1-\chi)\rho_B^H + \chi\rho_B^Q$ where χ is the fraction of quark matter and $1-\chi$ is the ratio of nuclear matter. Similarly, $\rho_3 = (1-\chi)\rho_3^H + \chi\rho_3^Q$ is the total isospin density.

As shown in the previous study, the phase transition features of asymmetric matter are isospin dependent. Once the species of heavy ions is chosen in HIC experiments, the asymmetry parameter will be determined. Due to the isospin conservation in strong interaction, the global asymmetry parameter α for the mixed phase,

$$\alpha \equiv -\frac{\rho_3}{\rho_B} = -\frac{(1-\chi)\rho_3^H + \chi\rho_3^Q}{(1-\chi)\rho_B^H + \chi\rho_B^Q}, \tag{16}$$

should maintain constant.

Although the global asymmetry parameter α keeps constant in the equilibrated state, in the coexisting phase the local asymmetry parameters, α^H and α^Q, can vary for different χ quark concentrations. It is just the χ dependence of α^H and α^Q that provides the possibility to test the isospin-relevant signals generated in the hadronization stage in HIC experiments. The details about the phase transformation from asymmetric nuclear matter to quark matter will be discussed in the next section. One can also refer to our previous research [70,74–76].

III. NUMERICAL RESULTS AND DISCUSSIONS

A. Features of pure quark matter in the EPNJL model with the entanglement interaction

First, in this subsection, we present some properties of pure quark matter in the EPNJL model. From Eq. (7), we can see that the value of α_1 and α_2 determines the strength of the entanglement between the chiral condensate and Poyakov loop. The PNJL model is just a special case of the EPNJL model with $\alpha_1 = 0$ and $\alpha_2 = 0$. In the PNJL model, the pseudocritical temperature of chiral restoration is $T_\sigma = 205.1$ MeV and that of color deconfinement is $T_\Phi = 172.7$ MeV at zero baryon chemical potential, as listed in Table II. The difference $\Delta = |T_\sigma - T_\Phi|/T_\sigma$ is about 15%. The coincidence predicted by the Coleman-Witten conjecture and other l-QCD simulations does not appear in the PNJL model without the entanglement interaction.

To show how the difference between the pseudocritical temperature of quark chiral restoration and that of color deconfinement varies with the strength of entanglement interaction, we calculate T_σ and T_Φ for several values of α_1 and α_2 at zero chemical potential. The same $T_0 = 210.0$ MeV, as used in the PNJL model, is adopted, and the numerical results are listed in Table II. This table clearly shows that the difference between T_σ and T_Φ gets smaller with the increase of α_1 and α_2. For the case of $\alpha_1 = \alpha_2 = 0.25$, the chiral restoration and deconfinement coincide. These results show the entanglement interaction is crucial for the coincidence of chiral restoration and deconfinement.

As a matter of fact, for the case of $\alpha_1 = \alpha_2 = 0.25$, $T_\Phi = 183.4$ MeV is out of the range $T_\Phi = 173 \pm 8$ MeV given

TABLE II. Pseudocritical temperatures of chiral restoration and deconfinement with different parametrization (α_1, α_2) of the entanglement interaction at zero baryon chemical potential with $T_0 = 210.0$ MeV.

α_1	α_2	T_σ	T_Φ	
0	0	205.1	172.7	PNJL
0.10	0.10	188.8	178.2	
0.15	0.15	185.0	180.9	EPNJL (A)
0.20	0.20	183.9	183.0	
0.25	0.25	183.4	183.4	

TABLE III. Pseudocritical temperatures of chiral restoration and deconfinement with $T_0 = 190.4$ MeV and the parametrization $(\alpha_1 = 0.2, \alpha_2 = 0.2)$.

α_1	α_2	T_σ	T_Φ	
0.20	0.20	173.0	173.0	EPNJL (B)

by l-QCD [7–9] and extracted from the data taken at RHIC [1]. Therefore, we take relatively smaller values of $\alpha_1 = \alpha_2 = 0.15$ with which the chiral restoration and deconfinement nearly coincide with $\Delta = |T_\sigma - T_\Phi|/T_\sigma \approx 2\%$, and T_Φ fulfill the requirement of l-QCD simulations. For convenience in later discussion, the parameter set with $\alpha_1 = \alpha_2 = 0.15$ is labeled "EPNJL (A)."

One alternative way to study the coincidence of chiral restoration and deconfinement is to reset T_0. With the parameters $T_0 = 190.4$ MeV, $\alpha_1 = \alpha_2 = 0.2$, the calculation shows $T_\sigma = T_\Phi = 173.0$ MeV, which means the coincidence appears and the corresponding pseudocritical temperatures are consistent with l-QCD and the experiment on RHIC. For this parameter set, we label it "EPNJL (B)" in Table III. Similar results can be obtained with $T_0 = 170$ MeV, but different cutoff Λ and coupling constant G [79].

With the parameter sets of the standard PNJL model, the EPNJL (A), and the EPNJL (B), we plot the chiral condensate ϕ_l/ϕ_{l0} $(\phi_l = \phi_u = \phi_d)$ and the Poyakov loop Φ as functions of T in Fig. 1. This figure shows that at low T the chiral condensate almost keeps constant, and the value of Φ is very close to zero. In this case, the entanglement interaction is very weak, which is easily understood from Eq. (7). For each parameter set of EPNJL(A) and EPNJL(B), this figure also demonstrates that there exists a range along temperature in which the chiral condensate decreases and Φ increases quickly. It implies that the entanglement effect between the chiral condensate and color confinement is strong in this range.

We calculate the partial derivatives of the chiral condensate $\partial\phi_l/\partial T$ and Poyakov loop $\partial\Phi/\partial T$ as shown in Fig. 2 for the different parameter sets. This figure and Fig. 1 demonstrate that the critical temperatures of the chiral condensate T_σ and color deconfinement T_Φ get close to each other when the entanglement interaction is included. In particular, for the parameter set of EPNJL(B), T_σ and T_Φ completely coincide.

In thermodynamics, the property of quark matter is highly relevant to the dynamical quark mass in the (P)NJL type models. With the inclusion of entanglement interaction, the dynamical quark mass M is determined by the product of $G(\Phi)$ and quark condensate ϕ_l, as given in Eq. (9). Therefore, the values of Φ and ϕ_l together (entangled through complex equations) are responsible for the dynamical quark mass, which just embodies the meaning of the entanglement interaction.

We should note that only when the values of both Φ and ϕ_l are not close to zero does the entanglement interaction play an important part. However, at very low temperatures, Φ is almost zero due to quark confinement, and at very high temperatures ϕ_l becomes small because of the chiral symmetry restoration. In the extreme low or high temperatures, the entanglement is weak, and the EPNJL model is almost equivalent to the PNJL model. When the temperature is in the range of about 160–200 MeV, neither Φ nor ϕ_l is small. In this case, the variation of Φ will affect the value ϕ_l and vice versa, due to the entanglement between them. It is just the entanglement interaction that provides the possibility of the coincidence of chiral restoration and deconfinement for appropriate parameters of α_1 and α_2. The numerical results demonstrated in Figs. 1 and 2 indeed prove this point.

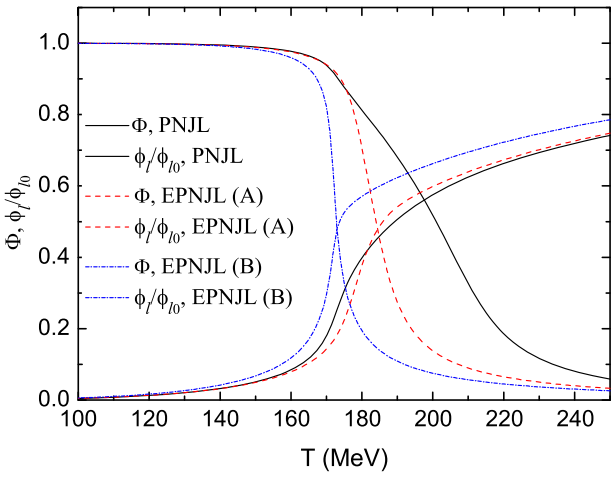

FIG. 1 (color online). ϕ_l/ϕ_{l0} and the Poyakov loop Φ as functions of T at zero chemical potential for the parameter sets of the standard PNJL model, the EPNJL (A), and the EPNJL (B).

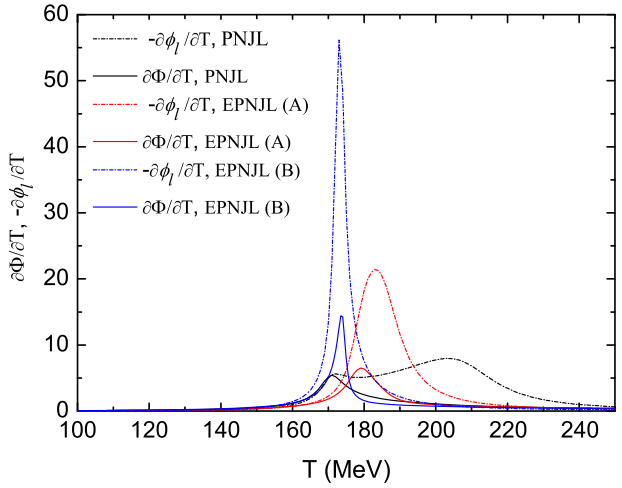

FIG. 2 (color online). Partial derivatives of the chiral condensate $-\partial\phi_l/\partial T$ and Poyakov loop $\partial\Phi/\partial T$ as functions of T at zero chemical potential for the parameter sets of the standard PNJL model, the EPNJL (A), and the EPNJL (B).

B. The phase transformation from nuclear to quark matter

In the above subsection, we present some properties of quark matter in the (E)PNJL quark model. In the following, we will show the phase transition from nuclear to quark matter based on the two-phase equilibrium theory. In this framework, the Gibbs criteria with more than one conserved charge are used. The transition signals are isospin dependent and are possibly measurable for asymmetric matter at the NICA and FAIR facilities [70,74–76]. The research in this part is focused on the phase transition from asymmetric matter to quark matter. Since the largest asymmetry parameter possibly reached for stable nuclei is the $\alpha = 0.227$ in $^{238}\mathrm{U} + ^{238}\mathrm{U}$ collision, we choose a reasonable value $\alpha = 0.2$ in the calculation to demonstrate the features of the phase transition. As a matter of fact, α can take a larger value for neutron-rich unstable nuclei.

First, in Fig. 3 we present the phase diagram of asymmetric matter in the T-ρ_B plane with the different parameter sets including the standard PNJL model, the EPNJL (A), and the EPNJL (B). From this figure, we see that the phase diagram for each parameter set is composed of three parts, the hadronic phase, the quark phase and the mixed phase. When the temperature is lower than 50 MeV, the phase diagrams derived by the three parameter sets are almost the same, but they are quite different at high temperatures. The reason is that the values of Φ and $\bar{\Phi}$ are almost zero at low temperatures, which leads to a very weak entanglement with the chiral condensate, but the entanglement increases with the rising Φ and $\bar{\Phi}$ at high temperatures close to pseudocritical points.

We can also see from Fig. 3 that there exists a critical end point (CEP) for each parameter set, close to the pseudocritical point predicted by l-QCD for smaller chemical potential. The locations of the critical end points depend on the entanglement interaction and the competition of dynamic mass of nucleons and quarks. As pointed out in our previous study [74], on the right side of the CEP, the effective nucleons mass; e.g., the proton mass, M_p derived in the hadronic phase is always larger than $M_u + 2M_d$ derived in the quark phase, and the relation $\rho_B^Q > \rho_B^H$ can be obtained for the hadron-quark phase transition. However, the effective mass of protons M_p in the hadronic phase is close to the value $M_u + 2M_d$ in the quark phase near the CEP, and $M_p < M_u + 2M_d$ will be derived on the left side of the CEP, which leads to $\rho_B^Q < \rho_B^H$, an unphysical solution. This is the reason why there exists a CEP in the two-EoS model when the dynamic quark masses are considered.

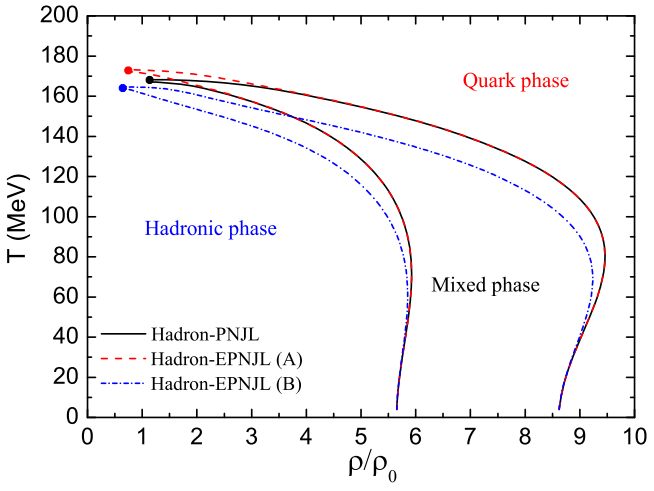

FIG. 3 (color online). Phase diagram of the hadron-quark phase transition in the T-ρ_B plane with the parameter sets of PNJL, EPNJL (A), and EPNJL (B).

Comparing the parameter set of the standard PNJL model with that of EPNJL(A), the only difference lies in the entanglement interaction which is included in the EPNJL(A) case. It is easy to see from Eq. (9) that the dynamic masses of quarks with the entanglement interaction in the EPNJL(A) are smaller than quark masses without this interaction for the same quark condensate at high temperature. Therefore, with the entanglement interaction the range in which $\rho_B^Q > \rho_B^H$ is enlarged, which explains why the CEP derived in the hadron-EPNJL(A) model moves to a smaller density and higher temperature than that of the hadron-PNJL model.

Similar behaviors appear in the hadron-EPNJL(B) results. Figure 3 also shows that the critical temperature of the hadron-EPNJL(B) is lower than that of the hadron-PNJL model. The reason is that a rescaled $T_0 = 190.4$ MeV is taken to get the coincidence of chiral restoration and deconfinement in the EPNJL(B) quark model. With $T_0 = 190.4$ MeV, the chiral restoration and deconfinement take place at relatively lower temperatures as presented in Figs. 1 and 2. When this parameter set is taken in the hadron-EPNJL(B) model, the pressure of the quark phase at the left of the CEP (along the baryon density) is larger than that of the hadron phase at high temperatures. In this case, the equilibrium cannot be reached. All of this explains the existence of a CEP with a smaller density and temperature in the hadron-EPNJL(B) model.

The phase diagram of the hadron-quark transformation in the T-μ_B plane is displayed in Fig. 4. Similar to Fig. 3, the phase diagram is composed of three parts for each parameter set. The lines with the same color show the boundaries of the pure hadronic and quark phase, and the corresponding intermediate part is the mixed range of nuclear and quark matter.

In Fig. 5, we display the hadronic and quark energy density at the boundaries of the hadron-quark phase transition. ε_H stands for the energy density of hadronic matter at the beginning of the phase transition, and ε_Q is the energy density of quark matter when only pure quark matter is observed. This figure shows a behavior similar to the $T - \rho_B$ phase diagram presented in Fig. 3. As discussed

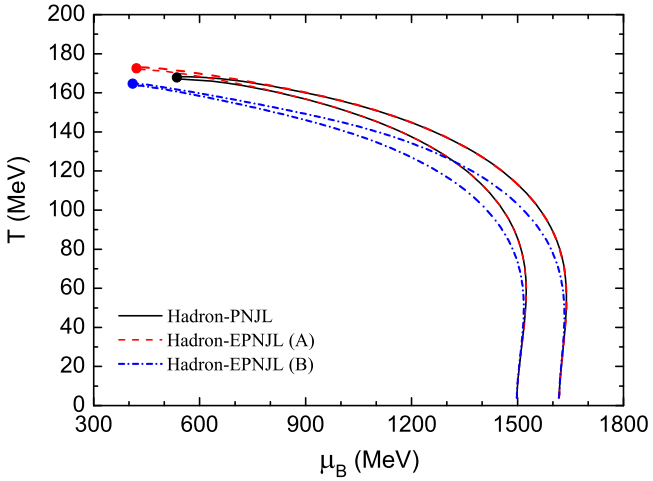

FIG. 4 (color online). Phase diagram of the hadron-quark phase transformaton in the T-μ_B plane with the parameter sets of PNJL, EPNJL (A), and EPNJL (B).

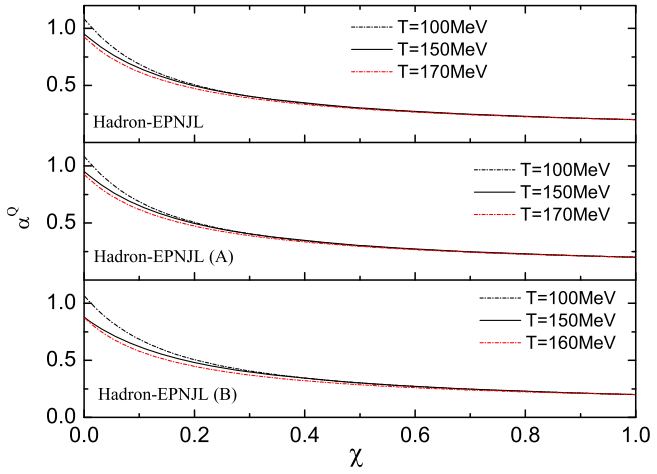

FIG. 6 (color online). Local isospin asymmetry parameter of α^Q inside the mixed phase at various temperatures with the parameter sets of PNJL, EPNJL (A), and EPNJL (B).

above, Fig. 5 indicates once again that the entanglement interaction plays an important role at high temperatures when both the chiral condensate and Φ vary quickly.

Finally we discuss the interesting isospin features of the phase transformation in the coexisting range. With the global asymmetry parameter $\alpha = 0.2$, we show in Fig. 6 the variation of the local isospin asymmetry parameters of α^Q as functions of quark fraction χ at different temperatures. We see that the value of α^Q is much larger at the beginning, when quark matter starts forming and χ is relatively small. We remark that α^Q will be further enhanced if a larger α is taken for unstable nuclei or an hadronic EoS with larger symmetry energy is taken as shown in [74,75].

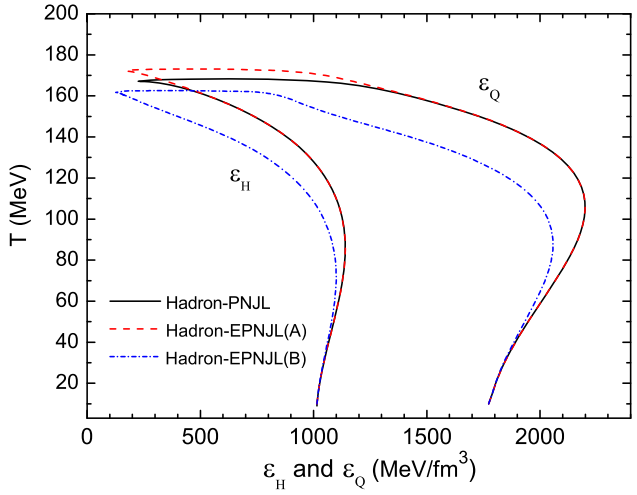

FIG. 5 (color online). Energy density ε_H of hadronic matter and ε_Q of quark matter at the boundaries of the hadron-quark phase transition with the parameter sets of PNJL, EPNJL (A), and EPNJL (B).

In the T-ρ_B plane as shown in Fig. 3, $\chi = 0$ starts from the left line for each parameter set. The values of α^Q decrease with the increase of quark concentration. The local asymmetry parameter α^Q reduces to the global asymmetry $\alpha = 0.2$ when the pure quark phase is reached with $\chi = 1$, which just embodies the isospin conservation in strong interaction. $\chi = 1$ corresponds to the right line in Fig. 3 for each parameter set. From Fig. 6, it appears that the behaviors of α^Q are the same with or without the entanglement interaction. This could be expected since the entanglement mechanism is not affecting the symmetry energy in the quark phase, which is behind the observed isospin distillation effect in the mixed phase [70,71,74–76].

Combining Figs. 3 and 4, we see that the transformation signals in the heavy-ion collision experiments are possibly quite different for different beam energy. When two beams collide, whether the hadron-quark phase transition can happen depends on the beam energy: (1) If the beams' energy is small, quark-gluon matter cannot forms. (2) If the beams' energy is high enough, pure quark-gluon matter can form. (3) For the intermediate beam energy, the beam energy can only transform a part of the nuclear matter into quark matter; i.e., the mixed phase but not the pure quark phase forms. A systematic analysis of nucleus-nucleus collisions in [68,69,80–82] shows that the hadron-quark-gluon mixed phase possibly forms in HIC experiments at intermediate energy.

Once the mixed phase is reached, due to the isospin conservation in the later hadronization stage, quarks will recombine into α^Q-dependent generated hadrons, i.e., also beam-energy-dependent. The different value of α^Q (or beam energy) will influence the isospin-relevant meson yield ratio, such as π^-/π^+, K^0/K^+. It also determines the production of isospin-rich resonances and subsequent decays. At the same time, nuclear matter that is not transformed into quark matter will emit neutron-rich

clusters, but due to the isospin trapping in the quark component of the mixed phase, the emission is greatly reduced as compared with the case of asymmetric matter without phase transition. Therefore, in the future facilities, we can perform the beam energy scan in a wide energy range and measure the relevant signals at RHIC, NICA, and FAIR, mapping isospin effects of generated hadrons. We can possibly discover the phase transition boundaries from nuclear to quark matter, and then also probe whether the entanglement interaction is strong or weak.

The vector interactions between quarks are not included in this study. In fact, we have discussed elaborately the role of vector interactions in the phase transition in our previous research [76]. The calculation shows that when the quark vector interactions are included, the features of the hadron-quark phase transition in the two-phase model are essentially preserved.

In particular, at high temperatures, the influence of vector interactions on the phase diagrams is minor. The reason is that the vector interactions mainly modify the effective quark chemical potential which is relevant to quark number density. However, from the $T-\mu_B$ and $T-\rho_B$ phase diagrams given by the two-phase model, we can see that both the chemical potential and quark number density are relatively small at high temperatures. Therefore, the modification to the phase diagram from vector interactions at high temperatures should be small as, in fact, obtained in the numerical calculations of [76].

At low temperatures, the inclusion of quark vector interactions will indeed affect the boundaries of the hadron-quark phase transition. Since the vector contributions are repulsive in both isoscalar and isovector channels, we can see two main effects. First, when the isoscalar vector interaction is considered, we have more repulsion in the quark sector and therefore the onset densities of the mixed phase at low temperatures will be postponed to higher values. The symmetry energy in the hadron phase will be larger, and so we will see a stronger isospin distillation, with an enhanced asymmetry parameter α_Q in the mixed phase. Second, when the isovector vector interaction is considered, the coexisting range at low temperatures will shrink, and α_Q in the mixed phase will decrease. This is because the isovector vector channel interaction is isospin relevant and enhances the symmetry energy of quark matter. As for how far the quark vector interactions will modify the phase diagram at low temperatures, that depends on the strength of vector coupling constants that have not yet been determined.

In conclusion, whether we include the vector interactions or not, the calculation in [76] shows that the main features of the phase diagram and phase-transition signature from asymmetric nuclear matter to quark matter are preserved. Moreover, experimental data on the mixed phase would also be relevant to shed light on the vector part of the quark interactions.

In fact, from the above analysis and the discussion about entanglement interaction contained in this study, we conclude that entanglement interaction plays an important role in the phase transition at high T and small μ_B, but the quark vector interactions are important at low T and large μ_B. Therefore, if we can map the isospin-relevant signals based on the full beam energy scan in the future, this will be helpful to understand both the entanglement interaction and the vector interactions between quarks.

IV. SUMMARY

We study the properties of quark matter at high temperature and the transformation from asymmetric nuclear matter to quark matter. In the description of quark matter, we take the recently developed EPNJL model in which the entanglement interaction between the chiral condensate and Poyakov loop is included. First, we discuss the coincidence of deconfinement and chiral restoration at zero baryon chemical potential. The calculation shows that the coincidence can happen by adjusting the strength of the entanglement interaction or by rescaling the value of T_0 in the effective potential $\mathcal{U}(\Phi,\bar{\Phi},T)$.

We further construct the hadron-EPNJL two-EoS model and use it to explore the phase transition from asymmetric nuclear matter to quark matter. We derived the boundaries of the phase transition for different parameter sets. Compared to the hadron-PNJL model, the calculation shows that the phase curves move to higher temperature and lower density if the entanglement interaction is considered and the same T_0 is used. However, if we rescale T_0 to a lower value with which the chiral restoration and deconfinement completely coincide in the pure EPNJL quark model, the phase transition curves move to slightly lower temperature and smaller density. According to the variation of local charge asymmetry α^Q with the increasing of quark concentration in the mixed phase and its dependence on beam energy, we suggest measuring some isospin-relevant signatures in the next generation accelerators such as FAIR and NICA, as well as in the BES program at RHIC, which would be helpful in understanding the entanglement interaction and restricting the value of T_0.

ACKNOWLEDGMENTS

This work is supported by the National Natural Science Foundation of China under Grant No. 11305121, the Specialized Research Fund for the Doctoral Program of Higher Education under Project No. 20130201120046, the Natural Science Basic Research Plan in the Shanxi Province of China (Program No. 2014JQ1012), and the Fundamental Research Funds for the Central Universities.

[1] S. Gupta, X. F. Luo, B. Mohanty, H. G. Ritter, and N. Xu, Science **332**, 1525 (2011).
[2] P. B. Demorest, T. Pennucci, S. M. Ransom, M. S. E. Roberts, and J. W. T. Hessels, Nature (London) **467**, 1081 (2010).
[3] J. Antoniadis *et al.*, Science **340**, 1233232 (2013).
[4] A. W. Steiner, J. M. Lattimer, and E. F. Brown, Astrophys. J. **765**, L3 (2013).
[5] P. Braun-Munzinger and J. Wambach, Rev. Mod. Phys. **81**, 1031 (2009).
[6] K. Fukushima and T. Hatsuda, Rep. Prog. Phys. **74**, 014001 (2011).
[7] F. Karsch, E. Laermann, and A. Peikert, Nucl. Phys. **B605**, 579 (2001).
[8] F. Karsch, Nucl. Phys. **A698**, 199 (2002).
[9] O. Kaczmarek and F. Zantow, Phys. Rev. D **71**, 114510 (2005).
[10] C. R. Allton, S. Ejiri, S. J. Hands, O. Kaczmarek, F. Karsch, E. Laermann, C. Schmidt, and L. Scorzato, Phys. Rev. D **66**, 074507 (2002).
[11] M. Cheng, N. H. Christ, S. Datta *et al.*, Phys. Rev. D **74**, 054507 (2006).
[12] Y. Aoki, S. Borsányi, S. Dürr, Z. Fodor, S. D. Katz, S. Krieg, and K. Szabo, J. High Energy Phys. 06 (2009) 088.
[13] Z. Fodor, S. D. Katz, and C. Schmidt, J. High Energy Phys. 03 (2007) 121.
[14] M. D'Elia and F. Sanfilippo, Phys. Rev. D **80**, 014502 (2009).
[15] S. Ejiri, Phys. Rev. D **78**, 074507 (2008).
[16] M. A. Clark and A. D. Kennedy, Phys. Rev. Lett. **98**, 051601 (2007).
[17] C. D. Roberts and A. G. Williams, Prog. Part. Nucl. Phys. **33**, 477 (1994).
[18] C. D. Roberts and S. M. Schmidt, Prog. Part. Nucl. Phys. **45**, S1 (2000).
[19] R. Alkofer and L. von Smekal, Phys. Rep. **353**, 281 (2001).
[20] C. S. Fischer, J. Phys. G **32**, R253 (2006).
[21] P. Maris and C. D. Roberts, Int. J. Mod. Phys. E **12**, 297 (2003).
[22] A. Bashir, L. Chang, I. C. Cloet, B. El-Bennich, Y. X. Liu, C. D. Roberts, and P. C. Tandy, Commun. Theor. Phys. **58**, 79 (2012).
[23] I. C. Clöt and C. D. Roberts, Prog. Part. Nucl. Phys. **77**, 1 (2014).
[24] S. S. Xu, Z. F Cui, B. Wang, Y. M. Shi, Y. C. Yang, and H. S. Zong, Phys. Rev. D **91**, 056003 (2015).
[25] T. Hatsuda and T. Kunihiro, Phys. Lett. B **145**, 7 (1984).
[26] S. P. Klevansky, Rev. Mod. Phys. **64**, 649 (1992).
[27] T. Hatsuda and T. Kunihiro, Phys. Rep. **247**, 221 (1994).
[28] R. Alkofer, H. Reinhardt, and H. Weigel, Phys. Rep. **265**, 139 (1996).
[29] M. Buballa, Phys. Rep. **407**, 205 (2005).
[30] P. Rehberg, S. P. Klevansky, and J. Hüfner, Phys. Rev. C **53**, 410 (1996).
[31] M. Huang and I. Shovkovy, Nucl. Phys. **A729**, 835 (2003).
[32] M. Alford, A. Schmit, K. Rajagopal, and T. Schäfer, Rev. Mod. Phys. **80**, 1455 (2008).
[33] P. C. Chu, X. Wang, L. W. Chen, and M. Huang, Phys. Rev. D **91**, 023003 (2015).
[34] G. Q. Cao, L. Y. He, and P. F. Zhuang, Phys. Rev. D **90**, 056005 (2014).
[35] D. P. Menezes, M. B. Pinto, L. B. Castro, P. Costa, and C. Providência, Phys. Rev. C **89**, 055207 (2014).
[36] J. Xu, T. Song, C. M. Ko, and F. Li, Phys. Rev. Lett. **112**, 012301 (2014).
[37] K. Fukushima, Phys. Lett. B **591**, 277 (2004).
[38] C. Ratti, M. A. Thaler, and W. Weise, Phys. Rev. D **73**, 014019 (2006).
[39] P. Costa, M. C. Ruivo, C. A. de Sousa, and H. Hansen, Symmetry **2**, 1338 (2010).
[40] T. K. Herbst, J. M. Pawlowski, and B-J. Schaefer, Phys. Lett. B **696**, 58 (2011).
[41] K. Kashiwa, H. Kouno, M. Matsuzaki, and M. Yahiro, Phys. Lett. B **662**, 26 (2008).
[42] H. Abuki, R. Anglani, R. Gatto, G. Nardulli, and M. Ruggieri, Phys. Rev. D **78**, 034034 (2008).
[43] W. J. Fu, Z. Zhang, and Y. X. Liu, Phys. Rev. D **77**, 014006 (2008).
[44] X. Y. Xin, S. X. Qin, and Y. X. Liu, Phys. Rev. D **89**, 094012 (2014).
[45] S. K. Ghosh, S. Raha, R. Ray, K. Saha, and S Upadhaya, Phys. Rev. D **91**, 054005 (2015).
[46] M. Dutra, O. Lourenço, A. Delfino, T. Frederico, and M. Malheiro, Phys. Rev. D **88**, 114013 (2013).
[47] B.-J. Schaefer, M. Wagner, and J. Wambach, Phys. Rev. D **81**, 074013 (2010).
[48] V. Skokov, B. Friman, and K. Redlich, Phys. Rev. C **83**, 054904 (2011).
[49] S. Chatterjee and K. A. Mohan, Phys. Rev. D **85**, 074018 (2012).
[50] Y. Sakai, T. Sasaki, H. Kouno, and M. Yahiro, Phys. Rev. D **82**, 076003 (2010).
[51] Y. Sakai, T. Sasaki, H. Kouno, and M. Yahiro, J. Phys. G **39**, 035004 (2012).
[52] T. E. Restrepo, J. C. Macias, M. B. Pinto, and G. N. Ferrari, Phys. Rev. D **91**, 065017 (2015).
[53] T. Sasaki,J. Takahashi, Y. Sakai, H. Kouno, and M. Yahiro, Phys. Rev. D **85**, 056009 (2012).
[54] T. Sasaki,Y. Sakai, H. Kouno, and M. Yahiro, Phys. Rev. D **84**, 091901(R) (2011).
[55] R. Gatto and M. Ruggieri, Phys. Rev. D **83**, 034016 (2011).
[56] M. Ferreira, P. Costa, and C. Providência, Phys. Rev. D **89**, 036006 (2014).
[57] N. K. Glendenning and S. A. Moszkowski, Phys. Rev. Lett. **67**, 2414 (1991); N. K. Glendenning, *Compact Stars* (Springer-Verlag, Berlin, 2000).
[58] N. K. Glendenning, Phys. Rev. D **46**, 1274 (1992).
[59] N. K. Glendenning and J. Schaffner-Bielich, Phys. Rev. Lett. **81**, 4564 (1998); Phys. Rev. C **60**, 025803 (1999).
[60] G. F. Burgio, M. Baldo, P. K. Sahu, and H.-J. Schulze, Phys. Rev. C **66**, 025802 (2002).
[61] T. Maruyama, S. Chiba, H-J. Schulze, and T. Tatsumi, Phys. Rev. D **76**, 123015 (2007).
[62] F. Yang and H. Shen, Phys. Rev. C **77**, 025801 (2008).
[63] G. Y. Shao and Y. X. Liu, Phys. Rev. C **82**, 055801 (2010); G. Y. Shao, Phys. Lett. B **704**, 343 (2011).
[64] J. Xu, L. W. Chen, C. M. Ko, and B. A. Li, Phys. Rev. C **81**, 055803 (2010).

[65] V. A. Dexheimer and S. Schramm, Phys. Rev. C **81**, 045201 (2010).
[66] G. Y. Shao, M. Colonna, M. Di Toro, Y. X. Liu, and B. Liu, Phys. Rev. D **87**, 096012 (2013).
[67] H. Müller, Nucl. Phys. **A618**, 349 (1997).
[68] M. Di Toro, A. Drago, T. Gaitanos, V. Greco, and A. Lavagno, Nucl. Phys. **A775**, 102 (2006).
[69] M. Di Toro, V. Baran, M. Colonna, G. Ferini, T. Gaitanos, V. Giordano, V. Greco, L. Bo, M. Zielinska-Pfabe, and S. Plumari, Prog. Part. Nucl. Phys. **62**, 389 (2009).
[70] M. Di Toro, B. Liu, V. Greco, V. Baran, M. Colonna, and S. Plumari, Phys. Rev. C **83**, 014911 (2011).
[71] B. Liu, M. Di Toro, G. Y. Shao, V. Greco, C. W. Shen, and Z. H. Li, Eur. Phys. J. A **47**, 104 (2011).
[72] R. Cavagnoli, C. Providência, and D. P. Menezes, Phys. Rev. C **83**, 045201 (2011).
[73] G. Pagliara and J. Schaffner-Bielich, Phys. Rev. D **81**, 094024 (2010).
[74] G. Y. Shao, M. Di Toro, B. Liu, M. Colonna, V. Greco, Y. X. Liu, and S. Plumari, Phys. Rev. D **83**, 094033 (2011).
[75] G. Y. Shao, M. Di Toro, V. Greco, M. Colonna, S. Plumari, B. Liu, and Y. X. Liu, Phys. Rev. D **84**, 034028 (2011).
[76] G. Y. Shao, M. Colonna, M. Di Toro, B. Liu, and F. Matera, Phys. Rev. D **85**, 114017 (2012).
[77] S. Rößner, C. Ratti, and W. Weise, Phys. Rev. D **75**, 034007 (2007).
[78] M. Fukugita, M. Okawa, and A. Ukava, Nucl. Phys. **B337**, 181 (1990).
[79] M. C. Ruivo, P. Costa, and C. A. de Sousa, Phys. Rev. D **86**, 116007 (2012).
[80] V. A. Kizka, V. S. Trubnikov, K. A. Bugaev, and D. R. Oliinychenko, arXiv:1504.06483v1.
[81] K. A. Bugaev, A. I. Ivanytskyi, D. R. Oliinychenko, V. V. Sagun, I. N. Mishustin, D. H. Rischke, L. M. Satarov, and G. M. Zinovjev, Phys. Part. Nucl. Lett. **12**, 238 (2015).
[82] K. A. Bugaev, A. I. Ivanytskyi, D. R. Oliinychenko, V. V. Sagun, I. N. Mishustin, D. H. Rischke, L. M. Satarov, and G. M. Zinovjev, arXiv:1412.0718.